Korean J. Chem. Eng., 40(9), 2312-2320 (2023)
DOI: 10.1007/s11814-022-1320-z

pISSN: 0256-1115
eISSN: 1975-7220

Correlation and thermal conductivity sensitivity analysis of ternary hybrid nanofluids containing CuO and TiO_2 nanoparticles and multi-walled carbon nanotubes

Mohammad Hemmat Esfe*,†, Soheyl Alidoust, and Davood Toghraie***,†**

*Nanfluid Advanced Research Team, Tehran, Iran
**School of Chemistry, Damghan University, Damghan, Iran
***Department of Mechanical Engineering, Khomeinishahr Branch, Islamic Azad University, Khomeinishahr,
(*Received 31 May 2022 • Revised 13 October 2022 • Accepted 19 October 2022*)

Abstract−The use of substandard nanofluids (NFs) in various industries causes the depreciation of industrial parts and shortens the life of the parts. Therefore, the researchers in this study will help to improve the performance of industrial equipment by preparing and examining a special hybrid nanofluid (HNF). The current research is divided into two experimental and theoretical parts. First, a ternary hybrid nanofluid (THNF) with three nanoparticles (NPs) CuO, MWCNT and TiO_2 with specific ratios and solid volume fraction (SVF) in water was prepared and produced. Then, the thermal conductivity (TC) of the produced nanofluid (NF) is measured by KD2 pro at different temperatures and SVFs. The results show that temperature and SVF are directly related to thermal conductivity enhancement (TCE). The maximum TC of the desired THNF is equal to 35.60% at SVF=1.65% and T=50 °C. In the theory part, using the response surface method (RSM), a very accurate correlation relationship R^2=0.9986 is provided. Also, the sensitivity of relative thermal conductivity (RTC) to changes of +10% SVF is presented, and the maximum deviation for the studied THNF is equal to 0.95%.

Keywords: Comparative Study, Thermal Conductivity, Ternary Hybrid Nanofluid (THNF), RSM, Nanoparticle, MWCNT, Mechanical Engineering, Nanotechnology, Heat Transfer

INTRODUCTION

It is safe to say that the transformation that nanotechnology has created in engineering sciences is unique, and for this reason, researchers have tried to use this new technology to improve various systems and have conducted much research in this field [1-8]. One of the most important aspects of the application of nanotechnology in fluids is heat transfer. In general, various applications can be defined for nanofluids such as lubrication, heat transfer, heat absorption, drilling and refinery industries [9-14]. Because additives to compounds, such as polymers, composites, and fluids, can significantly change their properties [15-20], the phenomenon of adding particles to fluids was followed years ago. In industrial applications, the fluid used in heating systems must have high TC, optimum viscosity and good convective heat transfer properties. Water, ethylene glycol (EG), or a mixture thereof and lubricating oils can be used as a coolant [21-23]. Understanding the thermal properties of these fluids plays a major role in the development and optimization of heat transfer equipment performance. Many methods can be used to increase heat transfer performance in a cooling environment. One of these is the use of microparticles (in millimeter, micrometer-scale) in thermal fluids. The use of these particles has created acceptable thermal advantages due to their higher heat capacity than conventional fluid. However, due to some problems due to particle size that causes abrasion of channel surfaces or fluid pressure drop that increases pumping costs, the use of this type of particle in industrial fluids has faced considerations. Therefore, researchers developed a new class of fluids called NFs by suspending metal or metal oxide NPs in fluids [24-27]. NFs are prepared from the suspension of NPs in ordinary fluids, which are known as a new group of smart fluids that can be used in various industries. A graphic design of hybrid nanofluid preparation is presented in Fig. 1. Qi et al. [28] investigated the natural convection characteristics of TiO_2/water NFs in a cavity filled with metal foam. The first study in the TC field of nanofluids was related to Maxwell. He reported the results of the study in question as a correlational analysis (Eq. (1)) [29].

$$RTC=\frac{k_{np}+2k_{bf}+2(k_{np}-k_{bf})}{k_{np}+2k_{bf}-(k_{np}-k_{bf})SVF} \quad (1)$$

The use of nanoscale particles in a pure base fluid was first proposed by Choi et al. [30] in 1995 to increase heat transfer as well as smooth out the problems of using mixtures containing millimeter and micrometer particles. Also, in an applied study [31], they investigated the effects of rotation angle and metal foam on the natural convection of NFs in a cavity under a magnetic field. They developed this concept and, as a result, called this solution NF. Recently, HNFs have attracted attention due to their better thermophysical properties compared to mono NFs [32-34]. HNFs can be defined as a combination of two or more types of NPs in a base fluid [35]. The use of hybrid particles can reduce production costs due to the high cost of using MWCNT as well as improve thermal properties. Many studies were conducted on the study of TC in which sev-

†To whom correspondence should be addressed.
E-mail: Toghraee@iaukhsh.ac.ir

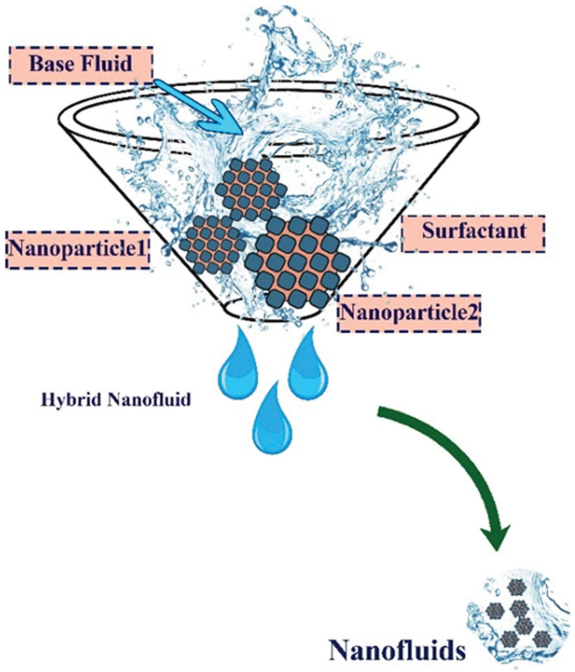

Fig. 1. Schematic of NF preparation.

eral factors affect its properties [36-39]. In experimental research [40], the thermophysical properties and heat transfer capacity of ZnO-MgO/engine oil HNFs as coolants and lubricants in various engineering applications were investigated. TC was measured at different temperatures (from T=15 °C to 55 °C) and SVF (from 0.125% to 1.5%). The maximum increase in TC of ZnO-MgO/engine oil HNFs was observed to be about 28% and 32% at T=55 °C and SVF=1.5%, respectively. NF samples are presented at different SVFs including 0.1-3%. different laboratory conditions are performed using the KD2 pro thermal analyzer, which uses a transient hot wire to measure TC. Findings show that the TC of NF increases with increasing SVF or temperature. Based on experimental data, a new correlation was proposed for modeling the TC of MgO/water (60%)-EG (40%) for different SVFs and temperatures. In Ref. [41], heat transfer and pressure drop of silver/ water NF in heat exchanger has been modeled using ANN modeling. The results show that R^2 for relative Nusselt number and pressure drop are 99.76% and 99.54%, respectively. Tables 1 and 2 provide an overview of past studies and results.

In this study, experimental research on the properties and TC of MgO (50%)-ZnO (35%) - MWCNT (15%)/water THNF in SVFs and different temperatures was carried out for the first time. Investigation of thermophysical properties with an emphasis on TC of THNFs will be done in the laboratory and RSM. Investigating TC using RSM allows researchers to obtain the TC correlation relationship with higher accuracy and speed. This study compares the effect of different temperatures and SVF on the TC of THNF. Also, the optimization of the target response was done using a mathe-

Table 1. Literature review of TC of HNFs

NPs	Base fluid	T (°C)	SVF (%)	Max TCE (%)	Ref.
MWCNT-CuO	Water	25-50	0.05-0.6	+30.38	Zadkhast et al. [27]
TiO_2	Water/EG	30-70	0.02-1	+44.5	Esfe [42]
TiO_2/MWCNT	Water/EG	25-50	0.05-1	+38.7	Akhgar et al. [43]
SiO_2	Ethanol	25-70	0.15-1.17	+9.5	Darvanjooghi et al. [44]

Table 2. Some of the researchers' past research and suggested correlations

Ref.	Correlation
Afrand et al. [45]	$\mathbf{TCR=(0.83411.1SVF^{+0.243}T^{-0.289})}$
Zadkhast et al. [27]	$\mathbf{TCR=[0.907exp(0.36SVF^{0.3111}+0.000956T)]}$
Alidoust et al. [46]	$\mathbf{TCR}$=0.96419-5.06469E-003$\mathbf{SVF}$+1.12712E-003 T+8.19160E-003$\mathbf{SVF}$ * T −6.07641E-003 SVF^2-3.54340E-003$\mathbf{SVF}^2$ T+0.030265$\mathbf{SVF}^3$
Parsian et al. [47]	$\mathbf{TCR}=\left(\frac{\mathbf{9.6128+SVF}}{\mathbf{9.3885-0.00010759T^2}}-\frac{\mathbf{0.0041}}{\mathbf{SVF}}\right)$
Esfe et al. [41]	$\mathbf{TC}$=0.4 +0.0332$\mathbf{SVF}$+0.00101T+0.000619$\mathbf{SVF}$ T+0.0687$\mathbf{SVF}^3$+ 0.0148$\mathbf{SVF}^5$−0.00218$\mathbf{SVF}^6$−0.0419$\mathbf{SVF}^4$−0.0604$\mathbf{SVF}^2$
Esfe et al. [48]	$\mathbf{TCR}$=1.01+0.007685$\mathbf{SVF}$ * $\mathbf{T}$−0.5136$\mathbf{SVF}^2\mathbf{T}^{-0.1578}$+11.5$\mathbf{SVF}^3\mathbf{T}^{-1.175}$
Vafaei et al. [49]	$\mathbf{TCR}$=0.9787+exp(0.3081$\mathbf{SVF}^{0.3097}$−$\mathbf{0.002T}$)

Table 3. Physical properties of NPs

NPs	Purity	APS	SSA	Color	True density
MWCNTs	>95 wt%	5-15 nm	233 /g	Black	~2.1 g/cm^3
TiO_2	99%	20 nm	10-45 m^2/g	White	g/cm^3
CuO	99%	40 nm	20 m^2/g	Black	6.4 g/m^3

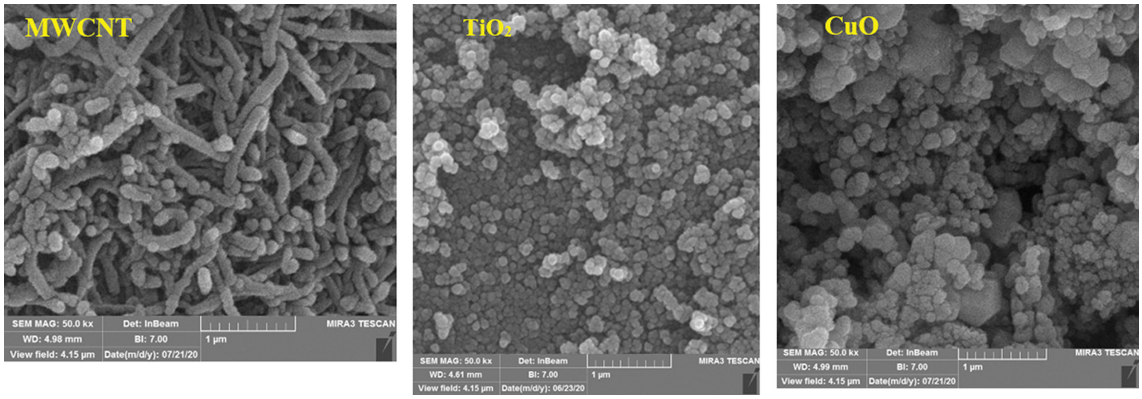

Fig. 2. SEM sample of NPs.

matical model. Sensitivity analysis and MOD were also used to evaluate the effect of SVF on TC.

EXPERIMENTAL PROCEDURE

1. Preparation of Samples

For the accurate thermal study of THNF, it is necessary to prepare with appropriate accuracy and quality. Initially, combinations of MWCNTs, TiO_2 and CuO NPs were used in proportions of 40%, 30% and 30% in water-based fluid, respectively. Table 3 shows the physical properties of NPs.

Advanced scanning electron microscope (SEM) and transmission electron microscope (TEM) imaging methods were used to identify the structural and morphological properties (size and shape) of the particles. Micrometer-scale imaging samples are shown in Fig. 2. Due to the uniqueness of the spectrum of each compound, it is possible to find the composition and formula of each unknown sample with the help of the XRD test in the laboratory. In Fig. 3, the wavelength spectrum of each nanoparticle is plotted by XRD. The powerful X'Pert Highscore software is used to analyze and identify the phases in the sample. This software uses the PDF-2 Powder Diffraction File database (which contains more than 160,000 graphs) as a reference to identify the phases in the sample. The mass values of each NP in the ratio of certain compounds to prepare HNFs in different SVFs can be determined from standard Eq. (2) [46] and then the mass of NPs is measured using a digital scale with an accuracy of 0.001 g.

$$\varphi = \frac{0.4\frac{w}{\rho}\Big|_{MWCNT} + 0.3\frac{w}{\rho}\Big|_{CuO} + 0.3\frac{w}{\rho}\Big|_{TiO_2}}{0.4\frac{w}{\rho}\Big|_{MWCNT} + 0.3\frac{w}{\rho}\Big|_{CuO} + 0.3\frac{w}{\rho}\Big|_{TiO_2} + \frac{w}{\rho}\Big|_{Water}} \times 100 \quad (2)$$

To prepare the HNFs, which is the first critical step in the experiments, we must ensure the proper dispersion of the NPs in the base fluid. In this way, suitable mechanisms such as agitation and ultrasound can be used to achieve the stability of the suspension against the deposition of NPs. A stirrer was used for the initial dispersion of the suspension mixture for three hours. Also, an ultrasonic vibration device was used for five hours for each of the SVFs to stabilize the stability and increase the quality of the NF. Fig. 4 shows a schematic of the NF preparation process.

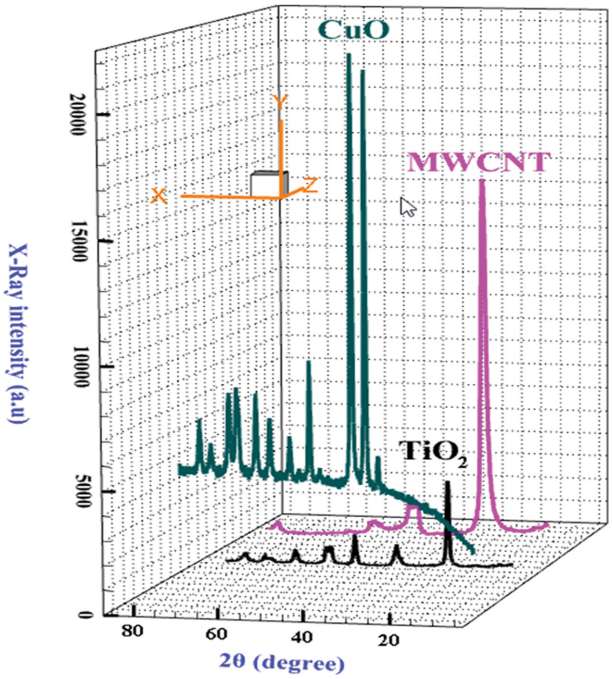

Fig. 3. XRD analysis of NPs.

2. Measurement of TC

KD2 Pro instrument was used to measure TC based on transient hot wire technique (Fig. 5). In this method, a KS-+1 stainless steel sensor with dimensions of 60 mm in length and 1.27 mm in diameter is used to measure TC. The measured TC range is 0.02 to 2.00 W/m·K with an accuracy of 0.01%. A water bath is used to control and stabilize the sample temperature during the measurement. In order to ensure the accuracy of the KD2 pro instrument, a comparison was made between the TC of pure water obtained by the KD2 pro at different temperatures and the TC of the ASHRAE handbook [50]. According to Fig. 6, the measurements are in good agreement with the available TC data. Because it was found that the difference in the mentioned temperature range is insignificant and less than 0.8%. To reduce the error and increase the quality of

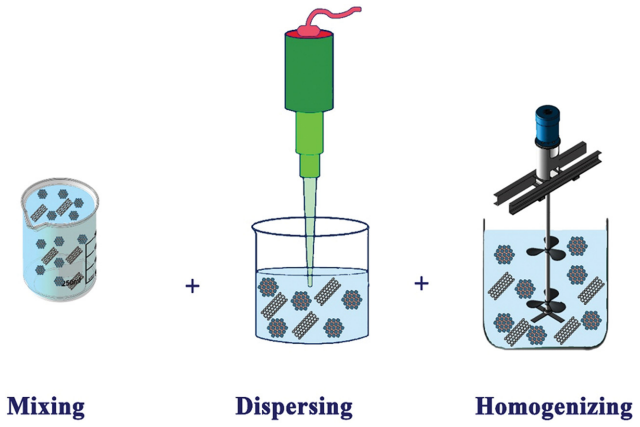

Fig. 4. Schematic of the NF stabilization process.

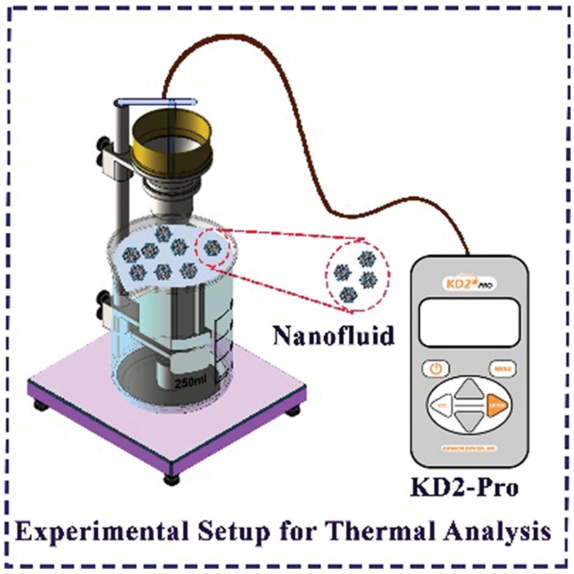

Fig. 5. Schematic of the KD2 pro device.

the results, all TC measurements were repeated three times and then their average was recorded, some of which are reported in Table 4. The interval between each measurement was set to 15 minutes.

RESULTS AND DISCUSSION

In this section, laboratory results are reviewed and analyzed. The effect of independent parameters of temperature and SVF on the TC of THNF was considered. The following is a detailed analysis of the TC of MWCNT-CuO-TiO_2/Water THNF.

1. RTC Versus SVF

The curves of RTC→SVF are shown in Fig. 7 to analyze the effect of the increasing trend of SVF on RTC. According to Fig. 8, the RTC improvement of the studied THNF is well observed after the addition of different SVFs. According to this curve, RTC increases in all SVFs (even in mild SVF=0.03% and 0.09%). Naturally, at higher SVFs, the RTC for THNF reaches its maximum value. It can be said that increasing the surface-to-volume ratio of NPs in

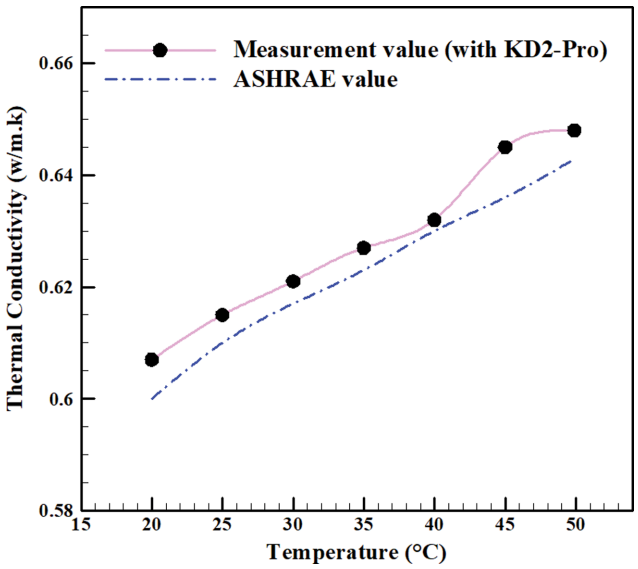

Fig. 6. Validation of KD2-pro (TC measurement device) results with ASHRAE results.

Table 4. Some laboratory results of the present study

HNF	SVF (%)	T (°C)	RTC
MWCNT(40%)-CuO(30%)-TiO_2(30%)/water	0.03	25	1.019
	0.09	30	1.029
	0.22	35	1.058
	0.45	40	1.121
	0.65	45	1.195
	0.9	50	1.250
	1.3	25	1.189
	1.65	50	1.356

THNF is possible after adding more NPs. The maximum RTC at T=50 °C and SVF=1.65% was equal to 35%.

2. TCE Versus Temperature

Fig. 8 shows the T→TCE curve, which shows the effect of temperature on the progress and recovery of TCE. According to the curve, the trend of increasing temperature has a positive effect on improving the TCE (%). It is normal for THNFs to reach their optimal TC at T=50 °C, that is, the highest temperature in this study. In a similar study in Ref. [20] for MWCNT-CuO/water HNF under the best study conditions, the amount of TCE did not exceed 30.38%. In this study, by adding the third NPs, i.e., TiO_2, this value reached 35.60% at T=50 °C. In addition to the significant improvement (22.5%) in TCE compared to this study, the use of TiO_2 NPs is more cost-effective and reasonable compared to the reasonably priced MWCNT. The TCE is obtained from Eq. (3) [46].

$$\text{TCE}\ (\%) = \left(\frac{k_{nf}}{k_{bf}} - 1\right) * 100 \tag{3}$$

Table 5 shows the TCE (%) values in all test conditions.

It is also possible to determine the influence of both temperature and SVF parameters for this study using the graphs in Fig. 9 and Table 5. But as mentioned, in the range of temperature and

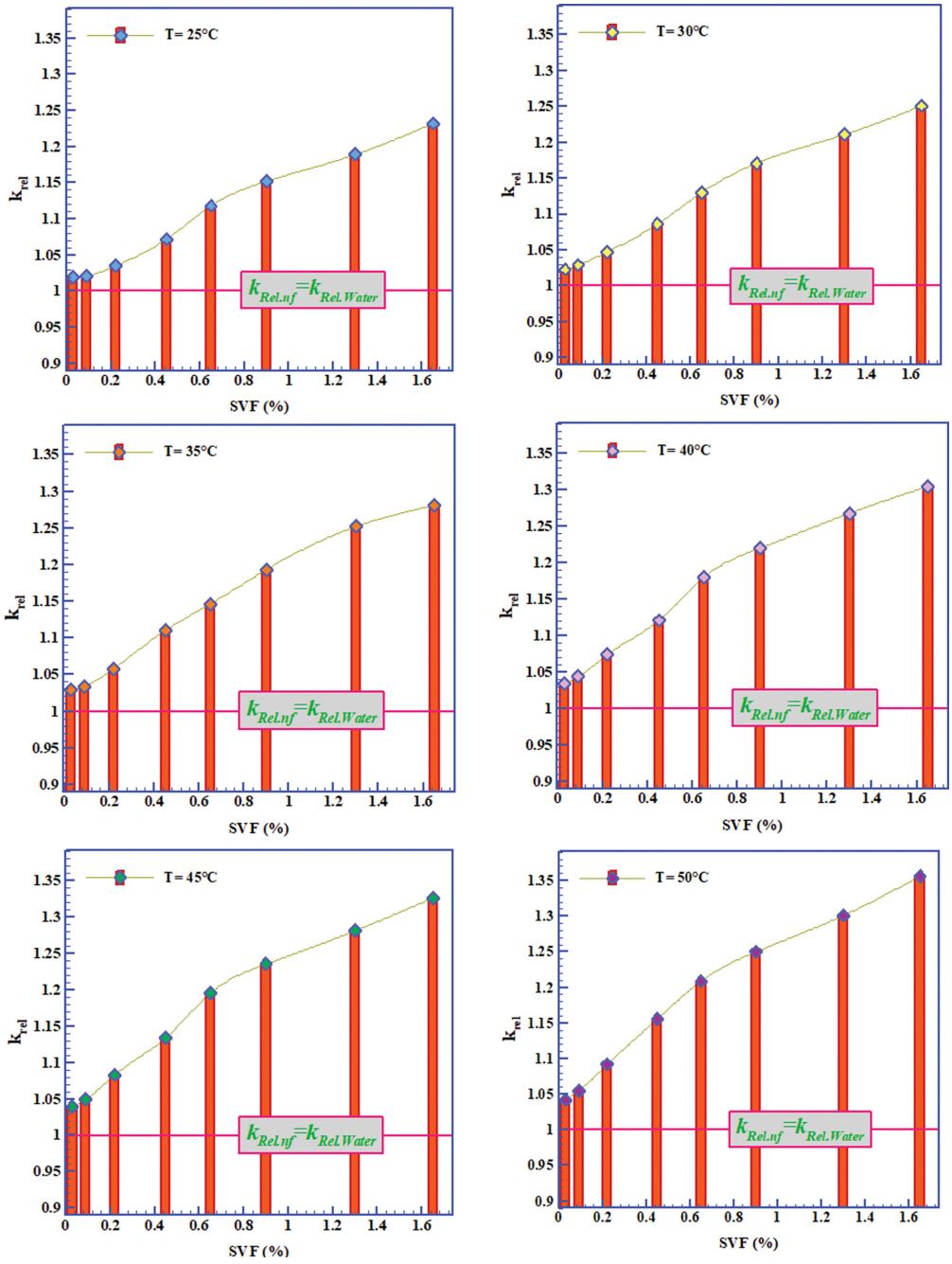

Fig. 7. RTC in terms of SVF.

Table 5. TCE (%) values in all test conditions

THNF	T (°C)	$\left(\frac{k_{nf}}{k_{bf}}-1\right)*100$							
		SVF=0.03%	0.09%	0.22%	0.45%	0.65%	0.9%	1.30%	1.65%
MWCNT (40%)-CuO (30%) TiO_2 (30%)/ Water	T=25	1.90	2.10	3.50	7.20	11.80	15.20	18.90	23.20
	T=30	2.30	2.90	4.70	8.60	13.00	17.10	21.10	25.10
	T=35	2.90	3.40	5.80	11.00	14.60	19.30	25.20	28.10
	T=40	3.50	4.40	7.40	12.10	18.00	22.00	26.80	30.50
	T=45	3.90	4.90	8.30	13.40	19.50	23.50	28.10	32.60
	T=50	4.20	5.50	9.20	15.60	20.90	25.00	30.10	35.60

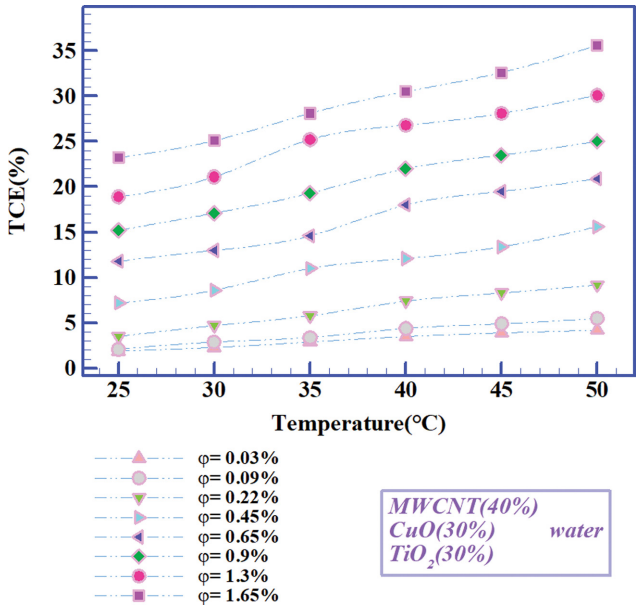

Fig. 8. TCE versus temperature.

SVF, the trend of TCE has been upward. As stated previously and detailed in Table 5, the maximum TCE was equal to 35.60%. Also, by keeping one parameter (for example, temperature or SVF) constant, the effect of another parameter can be checked. Here, the effect of SVF was more than temperature.

RESULTS OF RSM

In this section, RSM is considered to optimize the response function, provide a valid empirical model, and estimate the sensitivity of the response function to changes in the independent variable. The use of numerical methods helps researchers to obtain an accurate relation of dependent variables in the shortest time and with the least expense [51-56]. To predict the relationship between the input (temperature and SVF) and the output (TC) of the statistical model, the selected model with rank 4 was used. Table 6 shows the report of the ANOVA, based on the F-value; it can be said that the effect of the target response of the SVF variable is greater than that of the other parameters of the model. Table 7 shows the accuracy of the correlation model based on the R^2 coefficient. Considering the small difference between the parameters Adj R^2=0.9982 and Pred.R^2= 0.9978, as well as the high accuracy of the coefficient of determination R-Squared=0.9986, it can be concluded that the model has acceptable validity and quality.

Eq. (4) is proposed to predict the experimental data of MWCNT (40%)-CuO (30%)-TiO_2 (30%)/water THNF that can only be used in the laboratory. Eq. (4) can be used in sensitivity analysis as well as in determining the relationship between input and output variables in a statistical model.

$$\begin{aligned}RTC=&+1.02554+0.052804SVF-2.93004E\text{-}003\ T+4.94726E\text{-}003SVF\ T\\&+0.011774SVF^2+9.22629E\text{-}005\ T^2-1.24652E\text{-}003SVF^2\ T\\&-2.46023E\text{-}004SVF^3\ T+2.00463E\text{-}003SVF^4-1.27422E\text{-}008\ T^4\end{aligned}\quad (4)$$

According to Fig. 10, the acceptable adaptation of the modeled data to the experimental data on the bisector line shows the validity and capability of the model in data processing and forecasting.

1. Margin of Deviation (MOD)

To prove the correct correlation, the deviation analysis between the experimental data and the RSM outputs can be determined using Eq. (5) [46]. Exp and Pre subtitles show experimental data and RSM outputs, respectively. According to Fig. 11, the maximum proposed correlation deviation for the studied HNF is equal to

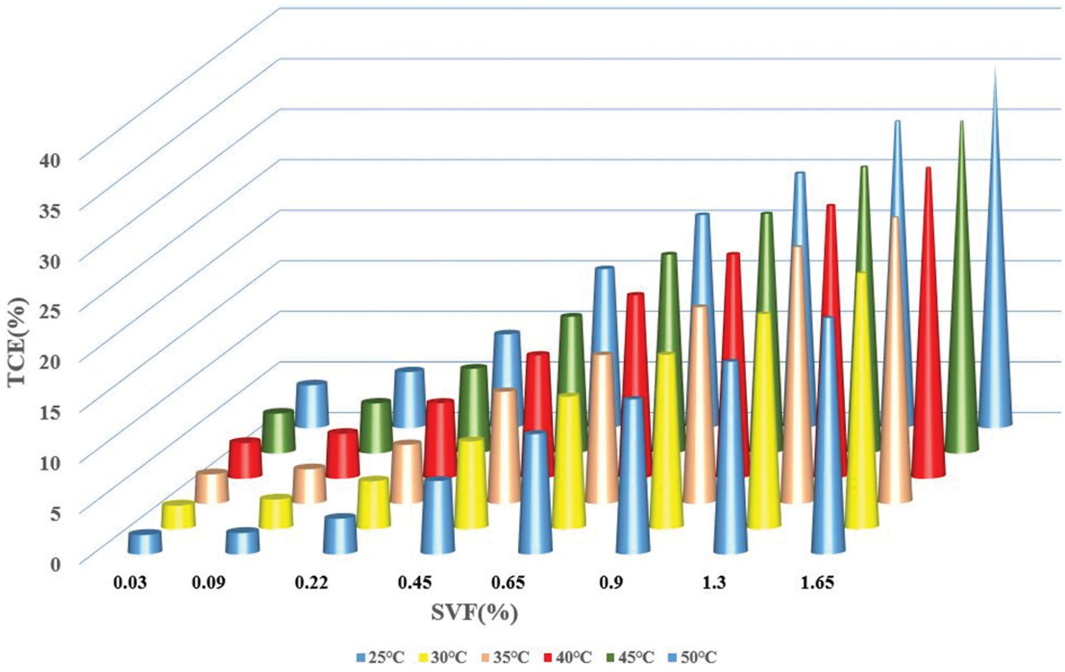

Fig. 9. Investigation of the simultaneous effect of temperature and SVF on RTC.

Table 6. ANOVA for response surface reduced quartic model

ANOVA table [Partial sum of squares - Type III]						
Source	Sum of squares	df	Mean square	F-value	P-value Prob>F	
Model	0.45	9	0.050	2,949.68	<0.0001	significant
A-SVF	0.35	1	0.35	20,915.93	<0.0001	
B-T	0.020	1	0.020	1,207.29	<0.0001	
AB	1.132E-004	1	1.132E-004	6.67	0.0138	
A^2	2.189E-003	1	2.189E-003	128.99	<0.0001	
B^2	1.006E-004	1	1.006E-004	5.93	0.0197	
A^2B	6.426E-004	1	6.426E-004	37.87	<0.0001	
A^3B	1.745E-004	1	1.745E-004	10.29	0.0027	
A^4	8.396E-004	1	8.396E-004	49.48	<0.0001	
B^4	7.429E-005	1	7.429E-005	4.38	0.0431	
Residual	6.448E-004	38	1.697E-005			
Cor total	0.45	47				

Table 7. Accuracy of model

Std. Dev.	4.119E-003	R^2	0.9986
Mean	1.14	Adj R^2	0.9982
C.V. (%)	0.36	Pred R^2	0.9978
PRESS	9.744E-004	Adeq Precision	178.960

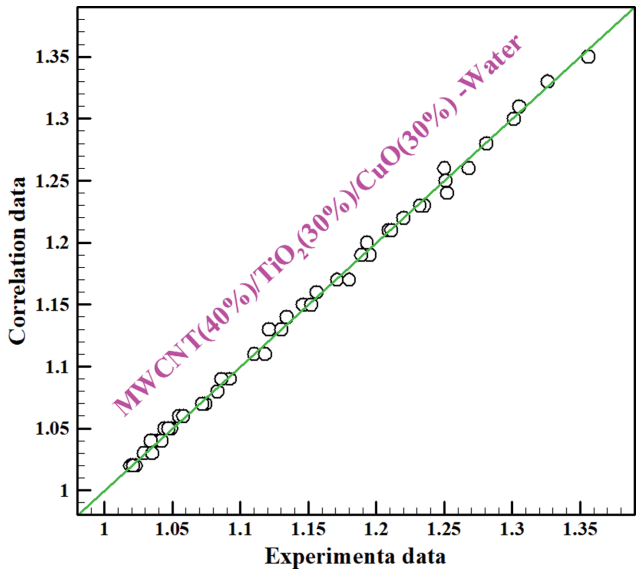

Fig. 10. Correlation of modeled data with experimental data.

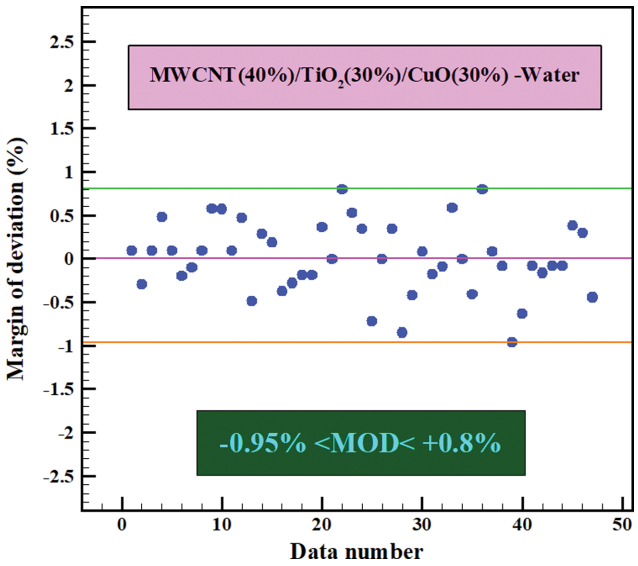

Fig. 11. MOD values.

0.95 %. According to Fig. 11, the deviation distribution is concentrated around zero, which means that the RSM model has good quality.

$$\mathrm{MOD}=\frac{\mathrm{RTC}_{exp}-\mathrm{RTC}_{pre}}{\mathrm{RTC}_{exp}}\times 100 \tag{5}$$

2. RTC Sensitivity

One of the most important applications of sensitivity analysis is to reduce the complexity of mathematical models by eliminating fewer effective parameters. In this study, only the estimation of the extent and effectiveness of RTC sensitivity to SVF changes is investigated. Eq. (6) [46] was used for sensitivity analysis. Fig. 12 reports the sensitivity to changes in the +10% increase in SVF factor. According to Fig. 12, the highest increase is observed in high SVFs, which occurred at T=50 °C and SVF=1.3%.

RTC sensitivity analysis

$$=\frac{(\mathrm{RTC}_{after\ change})_{Pre}-(\mathrm{RTC}_{before\ change})_{Pre}}{(\mathrm{TCR}_{before\ change})_{Pre}}\times 100 \tag{6}$$

CONCLUSIONS AND FUTURE DIRECTION

The use of substandard NFs prompts researchers to help improve the performance of industrial equipment by preparing and examining special HNFs. Hemmat Esfe research group hopes that the production of such HNFs with significant progress compared to HNFs of the same generation and high productivity can greatly help

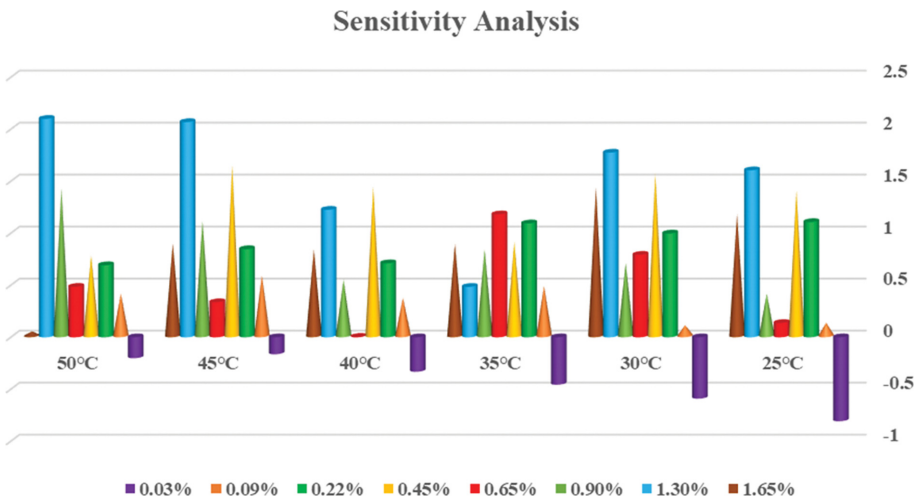

Fig. 12. Sensitivity analysis of TC in different SVFs.

industrialists to reduce their development problems. This study, using the RSM, in addition to accuracy, will save researchers time and energy. Based on RTC results, it increases in all research conditions and with increasing temperature and SVF. The maximum amount of TCE increase at T=50 °C and SVF=1.65% was equal to 35.60%. Compared to prepared NFs in past studies, the target NF has been able to further improve TC. Based on the results of the RSM, high accuracy of R-Squared=0.9986 has been achieved. The maximum MOD of the proposed correlation relation for THNF is equal to 0.95%. Finally, the sensitivity analysis of TC shows that the highest increase was observed in high SVFs, which occurred at T=50 °C and SVF=1.3%.

NOMENCLATURE

Abbreviation

Eq. : equation
N : number of measurements
NPs : nanoparticles
MWCNT : multi-walled carbon nanotubes
RSM : response surface methodology
RTC : relative thermal conductivity
S : standard deviation
SVF : solid volume fraction
XRD : X-ray diffraction
U : standard uncertainty
Xi : the measured value in each experiment
$\bar{x}$: average measured data

Greek Letters

ρ : density [kg/m^3]
φ : solid volume fraction

Latin Letters

C.V. % : coefficient of variation
k : thermal conductivity [W/(m·K)]
m : mass [kg]
W : molecular mass [kg/mol]

CONFLICT OF INTEREST STATEMENT

The authors declare that they have no known competing financial interests or personal relationships that could have appeared to influence the work reported in this paper.

REFERENCES

1. M. Mansouri, M. Nademi, M. Ebrahim Olya and H. Lotfi, *JCHR*, **7**(1), 19 (2017).
2. H. Dehghani Ashkezari, H. Sid Kalal, H. Hoveidi, M. R. Almasian and M. Ashoor, *CJES*, **15**(1), 1 (2017).
3. M. A. Asif, *JRSET*, **6**(04), 21 (2018).
4. N. K. A. Dwijendra, I. Patra, Y. M. Ahmed, Y. M. Hasan, Z. M. Najm, Z. I. Al Mashhadani and A. Kumar, *Monatsh. fur Chem.*, **153**(10), 873 (2022).
5. D. Domyati, *Eur. Chem. Bull.*, **11**(2), 1 (2022).
6. Y. Zhang, H. N. Li, C. Li, C. Huang, H. M. Ali, X. Xu, C. Mao, W. Ding, X. Cui, M. Yang, T. Yu, M. Jamil, M. K. Gupta, D. Jia and Z. Said, *Friction*, **10**, 803 (2022).
7. S. Alidoust, M. Zamani and M. Jabbari, *IJC*, **10**(4), 295 (2020).
8. Y. Wang, C. Li, Y. Zhang, M. Yang, B. Li, L. Dong and J. Wang, *Int. J. Precis. Eng. Manuf. - Green Technol.*, **5**(2), 327 (2018).
9. Z. Guo, J. Yang, Z. Tan, X. Tian and Q. Wang, *Int. J. Heat Mass Transf.*, **174**, 121296 (2021).
10. A. B. W. Putra, *Int. J. Inf. Commun. Technol.*, **8**(2), 9 (2020).
11. M. Yang, C. Li, Y. Zhang, D. Jia, X. Zhang, Y. Hou and J. Wang, *Int. J. Mach. Tools Manuf.*, **122**, 55 (2017).
12. M. Yang, C. Li, Y. Zhang, D. Jia, R. Li, Y. Hou and J. Wang, *Ceram. Int.*, **45**(12), 14908 (2019).
13. X. Cui, C. Li, Y. Zhang, W. Ding, Q. An, B. Liu, H. N. Li, Z. Said, S. Sharma, R. Li and S. Debnath, *Front. Mech. Eng.*, **18**, 3 (2023).
14. M. Liu, C. Li, Y. Zhang, Q. An, M. Yang, T. Gao and S. Sharma, *Front. Mech. Eng.*, **16**(4), 649 (2021).
15. J. Müssig and N. Graupner, *Progress in Adhesion and Adhesives*, **6**,

69 (2021).
16. M. Afrand, D. Toghraie and B. Ruhani, *Exp. Therm. Fluid Sci.*, **77**, 38 (2016).
17. H. Watandost, J. Achak and A. Haqmal, *IJIRMS*, **4**(4), 191 (2021).
18. B. Ruhani, M. Taheri Andani, A. M. Abed, N. Sina, G. Fadhil Smaisim, S. K. Hadrawi and D. Toghraie, *Heliyon*, **8**(11), e11373 (2022).
19. Y. F. Al-Khafaji, M. R. Al-Lami, A. S. Abbas, A. M. E. E. R. Al-Ameri and A. F. A. Mousa, *Asian J. Chem.*, **30**(2), 460 (2018).
20. S. Rostami, D. Toghraie, B. Shabani, N. Sina and P. Barnoon, *J. Therm. Anal. Calorim.*, **143**(2), 1097 (2021).
21. M. H. Esfe and A. A. A. Arani, *J. Mol. Liq.*, **259**, 227 (2018).
22. T. J. Choi, S. H. Kim, S. P. Jang, D. J. Yang and Y. M. Byeon, *J. Therm. Anal. Calorim.*, **180**, 115780 (2020).
23. S. E. Ghasemi, A. A. Ranjbar, M. J. Hoseini and S. Mohsenian, *J. Mater. Res. Technol.*, **15**, 2276 (2021).
24. T. Wen, G. Zhu, K. Jiao and L. Lu, *Int. J. Heat Mass Transf.*, **178**, 121617 (2021).
25. M. H. Esfe, M. K. Amiri and A. Alirezaie, *J. Therm. Anal. Calorim.*, **134**(2), 1113 (2018).
26. C. Qi, T. Chen, J. Tu and Y. Yan, *Int. J. Energy Res.*, **44**(13), 10628 (2020).
27. M. Zadkhast, D. Toghraie and A. Karimipour, *J. Therm. Anal. Calorim.*, **129**(2), 859 (2017).
28. G. Wang, C. Qi and J. Tang, *J. Therm. Anal. Calorim.*, **141**(1), 15 (2020).
29. J. C. Maxwell, *Clarendon Press*, 1 (2008).
30. S. U. Choi and J. A. Eastman, Argonne National Lab. (ANL), Argonne, IL (United States) (1995).
31. C. Qi, J. Tang, Z. Ding, Y. Yan, L. Guo and Y. Ma, *Int. Commun. Heat Mass Transf.*, **109**, 104349 (2019).
32. M. H. Esfe, H. Rostamian and M. R. Sarlak, *J. Mol. Liq.*, **254**, 406 (2018).
33. A. Asadi, A. N. Bakhtiyari and I. M. Alarifi, *Eng. Comput.*, **37**(4), 3813 (2021).
34. H. Adun, D. Kavaz, M. Dagbasi, H. Umar and I. Wole-Osho, *Powder Technol.*, **394**, 1121 (2021).
35. K. Y. Leong, K. K. Ahmad, H. C. Ong, M. J. Ghazali and A. Baharum, *Renew. Sustain. Energy Rev.*, **75**, 868 (2017).
36. Z. Tang, C. Qi, L. Zhang and Z. Tian, *Transp. Porous Media*, **142**, 599 (2022).
37. T. Ambreen and M. H. Kim, *Appl. Energy*, **264**, 114684 (2020).
38. Z. Li, R. Kalbasi, Q. Nguyen and M. Afrand, *Powder Technol.*, **367**, 464 (2020).
39. A. Moradi, M. Zareh, M. Afrand and M. Khayat, *Powder Technol.*, **362**, 578 (2020).
40. A. Asadi and F. Pourfattah, *Powder Technol.*, **343**, 296 (2019).
41. M. H. Esfe, *Appl. Therm. Eng.*, **126**, 559 (2017).
42. M. Hemmat Esfe, *J. Therm. Anal. Calorim*, **127**(3), 2125 (2017).
43. A. Akhgar and D. Toghraie, *Powder Technol.*, **338**, 806 (2018).
44. M. H. K. Darvanjooghi and M. N. Esfahany, *Int. Commun. Heat Mass Transf.*, **77**, 148 (2016).
45. M. Afrand, *Appl. Therm. Eng.*, **110**, 1111 (2017).
46. S. Alidoust, F. AmoozadKhalili and S. Hamedi, *Colloids Surf. A: Physicochem. Eng. Asp.*, **645**, 128625 (2022).
47. A. Parsian and M. Akbari, *J. Therm. Anal. Calorim.*, **131**(2), 1605 (2018).
48. M. Hemmat Esfe, S. Esfandeh and M. Rejvani, *J. Therm. Anal. Calorim.*, **131**(2), 1437 (2018).
49. M. Vafaei, M. Afrand, N. Sina, R. Kalbasi, F. Sourani and H. Teimouri, *Phys. E: Low-Dimens. Syst. Nanostructures*, **85**, 90 (2017).
50. D. J. Thevenard and R. G. Humphries, *ASHRAE Trans.*, **111**, 457 (2005).
51. F. Ahmad, *CAAI Trans. Intell. Technol.*, **7**(2), 200 (2022).
52. J. Khan, E. Lee and K. Kim, *CAAI Trans. Intell. Technol.*, 1 (2022).
53. C. Deng, L. Zhang and H. Deng, *CAAI Trans. Intell. Technol.*, **7**(2), 268 (2022).
54. S. Sharma, K. Verma and P. Hardaha, *J. Comput. Cognitive Eng.*, **2**(2), 155 (2023).
55. Z. Chen, *J. Comput. Cognitive Eng.*, **1**(3), 103 (2022).
56. R. Hanif, S. Mustafa, S. Iqbal and S. Piracha, *J. Comput. Cognitive Eng.*, **2**(2), 143 (2023).